色素上皮細胞に対する集積を測定するために、多数のレーザー光凝固術を行い、3 日後に色素上皮・脈絡膜を取り出して F4/80 で染色して、フローサイトメトリーにより検出した。またレーザー後の経時的な IL-10 の発現を同様に ELISA により測定した。

（倫理面への配慮）

動物実験の取り扱いは ARVO に準じた。

C．研究結果

対照、IL-10 の 0.5ng および 5ng 投与群の CNV の面積は、それぞれ 26.65±16.23、21.74±3.60、12.61±4.80、（$\times 10^3$ um^2）であった（図 1）。また VEGF の発現はそれぞれ、48.74± 10.7 、41.68±8.3 、22.36±4.32（pg/mg protein）であった（図 2）。マクロファージの集積(Index)はそれぞれ、1.0、1.08±0.23、0.60±0.12 であった（図 3）。レーザー光凝固術後いずれの時期においても IL-10 の発現は認められなかった。

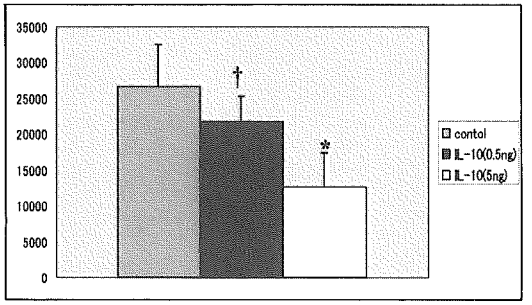

(† P=0.16, * P =0.0004. N = 30 for all groups.)

図１　各群の CNV 面積（um^2 ）IL-10 の 0.5ng 投与群では抑制効果はないが、5ng 投与群では対照と比較して有意に CNV 生成が抑制されている。

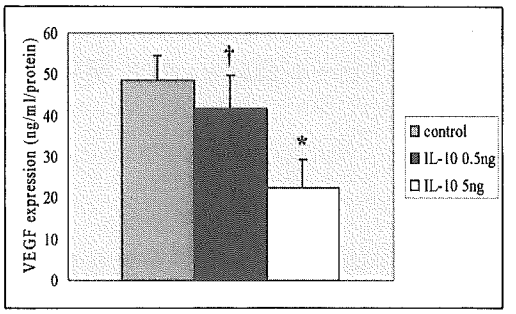

(† P=0.105, * P =0.0015. N = 12 for all groups.)

図２　各群のレーザー3 日後の VEGF 発現量（pg/mg protein）　IL-10 の 0.5ng 投与群は VEGF の有意な抑制効果はないが、5ng 投与群では有意に VEGF 発現の抑制効果がみられる。

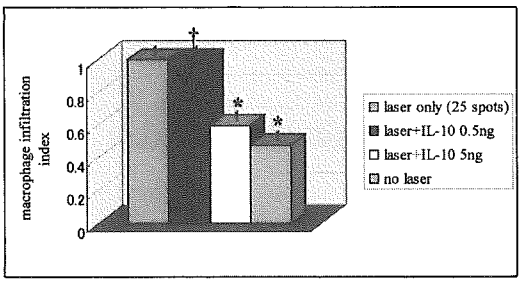

(† P=0.84, * P <0.01. N = 4 for all groups.)

図３　各群のレーザー光凝固 3 日後のマクロファージ集積（Index）（* P ＜ 0.01）IL-10 の 5ng 投与群では色素上皮・脈絡膜に対するマクロファージの集積抑制を認める。

D．考察

IL-10 は抗炎症性サイトカインでマクロファージの活性と遊走を抑制するとされている[4－5]。また近年では血管新生抑制効果[6]、抗腫瘍性効果を有すると報告されている。今回、我々の結果では IL-10 はレーザーによる CNV の生成を有意に抑制した。機序と

してマクロファージの色素上皮・脈絡膜への集積抑制が考えられた。CNV の抑制効果はマクロファージ集積と VEGF 発現量に相関していた。

E．結論

IL-10 硝子体投与は脈絡膜新生血管の治療に有用である可能性が示唆された。

F．健康危険情報

なし

G．研究発表

1．論文発表

なし

2．学会発表

なし

H．知的財産権の出願・登録状況

1．特許取得

なし

2．実用新案登録

なし

3．その他

なし

I．参考文献

1. Anderson DH et al: A role for local inflammation in the formation of drusen in the aging eye. Am J Ophthalmol, 134: 411-431, 2002.
2. Sakurai E et al: Targeted disruption of the CD18 or ICAM-1 gene inhibits choroidal neovascularization. Invest Ophthalmol Vis Sci 27:43-2749, 2003.
3. Sakurai E et al: Macrophage depletion inhibits experimental choroidal neovascularization. Invest Ophthalmol Vis Sci, 44: 3578-3585, 2003.
4. O'Farrell AM et al: IL-10 inhibits macrophage activation and proliferation by distinct signaling mechanisms: evidence for Stat3-dependent and -independent pathways. EMBO J. 17(4):1006-1018, 1998.
5. Williams L et al: Signal transducer and activator of transcription 3 is the dominant mediator of the anti-inflammatory effects of IL-10 in human macrophages.J Immunol. 172(1):567-576, 2004.
6. Silvestre JS: Antiangiogenic effect of interleukin-10 in ischemia-induced angiogenesis in mice hindlimb. Circ Res.87(6): 448-52, 2000.

44. アトルバスタチンによる実験的脈絡膜新生血管抑制効果

山田　潔、櫻井英二、山崎　哲、板谷正博、小椋祐一郎
(名古屋市大)

研究要旨　HMG CoA 還元酵素阻害剤であるアトルバスタチン投与による、レーザー誘発の脈絡膜新生血管 (choroidal neovascularization, CNV) の抑制効果を検討した。
雄の生後約 6 週の C57BL/6J マウスに、アトルバスタチン 10 mg/kg/day または 20 mg/kg/day を、レーザー網膜光凝固を行う前後 3 日間、計 6 日間投与した。1 週間後に眼球摘出、fluorescein isothiocyanate (FITC)-lectin B4 で染色してフラットマウントを作成し、共焦点顕微鏡で CNV の面積を測定し比較検討した。また、凝固 3 日後に網膜色素上皮・脈絡膜での血管内皮増殖因子 (vascular endothelial growth factor, VEGF) の発現を ELISA により測定し比較検討した。さらに、同時期に網膜色素上皮・脈絡膜に集積したマクロファージを F4/80-Cy5 で染色し、フローサイトメトリーで検出、比較検討した。アトルバスタチンを投与した群はいずれもレーザー誘発の CNV が有意に抑制された。同様に、アトルバスタチンを投与した群はいずれも VEGF の発現量およびマクロファージの集積が有意に抑制された。アトルバスタチン投与により VEGF の発現およびマクロファージの集積が抑制され、レーザー誘発の CNV が抑制されたと考えられた。

A. 研究目的

近年、加齢黄斑変性の原因として、炎症が注目されている [1, 2]。加齢黄斑変性の前駆病変とされるドルーゼンの組成が、リポフスチン、IgG、アミロイド、補体などの炎症起因物質であることが判明したためである。また、我々はマクロファージを減少させるとレーザー誘発の脈絡膜新生血管を有意に抑制されることを報告 [3] し、脈絡膜新生血管の生成とマクロファージには密接な関係があることが明らかになってきた。

一方、高脂血症の治療薬として広く使用されている HMG CoA 還元酵素阻害剤は、近年その多面発現効果として抗血管新生作用 [4] や抗炎症作用 [5] が注目されている。そこで我々は、HMG CoA 還元酵素阻害剤の一種であるアトルバスタチンをマウスに投与し、レーザー誘発の脈絡膜新生血管の抑制効果を検討した。

B. 研究方法

雄の生後約 6 週の C57BL/6J マウスにアトルバスタチン 10 mg/kg/day (10 mg 投与群) または 20 mg/kg/day (20 mg 投与群) をレーザー光凝固の前後 3 日間、計 6 日間経口投与した。

視神経周囲にレーザー網膜光凝固 (200mW、100μm、100ms、532nm) を 4 発行い、1 週間後に眼球を摘出して fluorescein isothiocyanate (FITC)-lectin B4 で染色しフラットマウントを作成し、共焦点顕微鏡で CNV の面積を測定し比較検討した。ま

た Vascular Endothelial Growth Factor (VEGF) の発現を比較検討するため、同条件で25発のレーザー網膜光凝固を行い、3日後に眼球を取り出し脈絡膜・網膜色素上皮を分離し、各群を ELISA により測定した。さらに脈絡膜・網膜色素上皮に集積したマクロファージを測定するため、同条件で25発のレーザー網膜光凝固を行い、3 日後に眼球を摘出、脈絡膜・網膜色素上皮を取り出し F4/80-Cy5 で染色して、フローサイトメトリーにより検出した。

(倫理面への配慮)

実験動物の取り扱いは ARVO に準じた。

C. 研究結果

対照群、10 mg 投与群、20 mg 投与群の CNV の面積は、それぞれ 26.57±3.18、11.25±2.35、13.73±3.36 ($\times 10^3\ \mu m^2$) であった (図1)。また VEGF の発現は、それぞれ 47.55± 7.18、29.60±3.46、24.16±7.03 (pg/mg protein) であった (図2)。マクロファージの集積は、それぞれ 4.33±1.55、1.32±0.23、1.14±0.33 (%) であった (図3)。

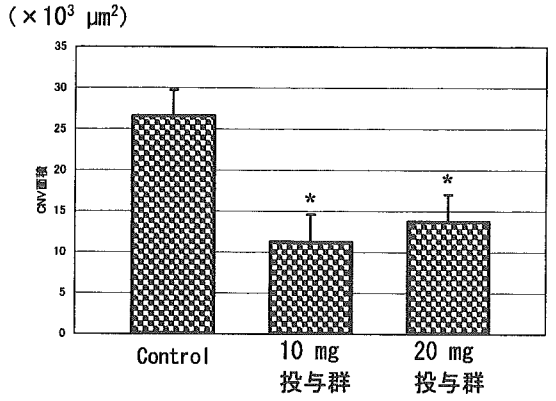

図1 各群の CNV 面積 (μm^2) (*P<0.01)

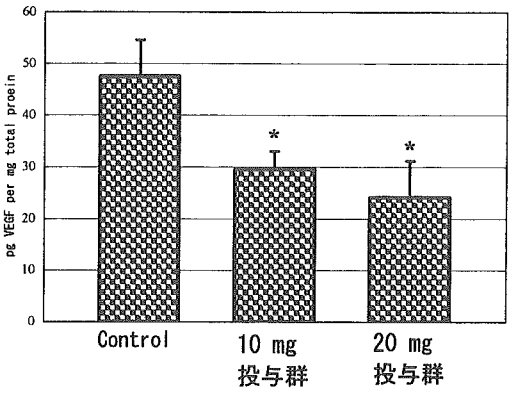

図2 各群のレーザー網膜光凝固3日後の VEGF 発現量 (pg/mg protein) (*P<0.01)

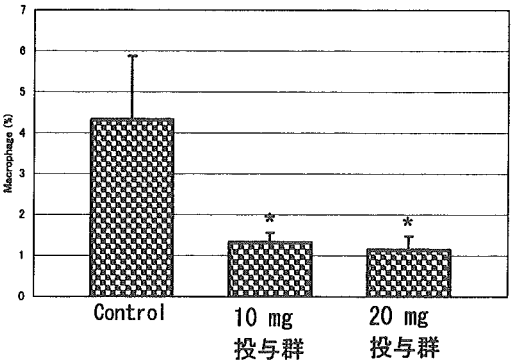

図3 各群のレーザー網膜光凝固3日後のマクロファージ集積 (%) (*P<0.05).

D. 考察

アトルバスタチンを投与しレーザー誘発の脈絡膜新生血管が抑制されたが、10 mg 投与群と 20 mg 投与群では有意差はなかった。VEGF 発現量、マクロファージの脈絡膜・網膜色素上皮への集積の結果も同様であり、今回の実験系ではアトルバスタチン 10 mg/kg/day の投与量で十分に効果が現れていたと考えられる。VEGF 発現量、マクロファージの集積の結果は一致しており、脈絡膜新生血管発症過程においてもマクロファージが主な VEGF の源であることが示唆さ

れた。

E．結論

アトルバスタチン投与は、レーザー誘発の脈絡膜新生血管を有意に抑制した。その機序としてマクロファージの遊走阻害およびVEGFの発現抑制が示唆された。

F．健康危険情報

なし

G．研究発表

1．論文発表

なし

2．学会発表

1. Yamada K et al. Atorvastatin inhibits laser-induced experimental choroidal neovascularization through downregulation of vascular endothelial growth factor. The Association for Research in Vision and Ophthalmology (ARVO), Fort Lauderdale, Florida, 2006.

H．知的財産権の出願・登録状況

1．特許取得

なし

2．実用新案登録

なし

3．その他

なし

I．参考文献

1. Anderson DH et al: A role for local inflammation in the formation of drusen in the aging eye. Am J Ophthalmol, 134: 411-431, 2002.
2. Sakurai E et al: Targeted disruption of the CD18 or ICAM-1 gene inhibits choroidal neovascularization. Invest Ophthalmol Vis Sci, 44: 2743-2749, 2003.
3. Sakurai E et al: Macrophage depletion inhibits experimental choroidal neovascularization. Invest Ophthalmol Vis Sci, 44: 3578-3585, 2003.
4. Cooke JP et al: Statins have biphasic effects on angiogenesis. Circulation 105: 739-745, 2002.
5. Inoue I et al: Lipophilic HMG-CoA reductase inhibitor has an anti-inflammatory effect: reduction of MRNA levels for interleukin-1beta, interleukin-6, cyclooxygenase-2, and p22phox by regulation of peroxisome proliferator- activated receptor alpha (PPARalpha) in primary endothelial cells. Life Sci 67: 863-876, 2000.

Macrophage Depletion Inhibits Experimental Choroidal Neovascularization

Eiji Sakurai,[1] *Akshay Anand,*[1] *Balamurali K. Ambati,*[2] *Nico van Rooijen,*[3] *and Jayakrishna Ambati*[1]

OBJECTIVE. To investigate the role of macrophages in the development of laser-induced choroidal neovascularization (CNV) by selective depletion with liposomal clodronate (Cl_2MDP-LIP).

METHODS. Laser photocoagulation was used to induce CNV in wild-type C57BL/6J mice. Animals were treated with intravenous (IV) and/or subconjunctival (SC) Cl_2MDP-LIP or PBS-LIP at the following time points: 2 days before, immediately after, 2 days before and immediately after, or 2 days after laser injury. CNV responses were compared on the basis of en masse volumetric measurements and fluorescein angiography after laser photocoagulation. Macrophages were identified by immunostaining for F4/80, and vascular endothelial growth factor (VEGF) expression was quantified by ELISA.

RESULTS. Macrophages invaded the site of laser injury within 1 day of photocoagulation and peaked at 3 days. IV Cl_2MDP-LIP significantly decreased the volume of CNV and angiographic leakage when administered 2 days before and/or immediately after laser injury, but not when administered 2 days after injury. SC Cl_2MDP-LIP significantly decreased lesion volume when coadministered with IV PBS-LIP but not IV Cl_2MDP-LIP. IV Cl_2MDP-LIP was significantly more beneficial when administered 2 days before laser injury than immediately after, but combining SC Cl_2MDP-LIP with IV treatment eliminated this difference. Reduction in CNV volume correlated with VEGF protein levels and number of infiltrating macrophages.

CONCLUSIONS. Generalized macrophage depletion reduced the size and leakage of laser-induced CNV and was associated with decreased macrophage infiltration and VEGF protein. These findings define the role of the macrophage as a critical component in initiating the laser-induced CNV response. (*Invest Ophthalmol Vis Sci.* 2003;44:3578-3585) DOI:10.1167/iovs.03-0097

From the [1]Department of Ophthalmology, University of Kentucky, Lexington, Kentucky; the [2]Department of Ophthalmology, Medical College of Georgia, Augusta, Georgia; and the [3]Department of Cell Biology and Immunology, Vrije Universiteit, Amsterdam, The Netherlands.

Supported by Career Development Awards from Foundation Fighting Blindness (JA) and American Geriatrics Society (JA), a Prevent Blindness America/Fight for Sight Grant-in-Aid (JA), the University of Kentucky Physician Scientist Award (JA), and Knights-Templar Eye Foundation (BKA).

Submitted for publication January 29, 2003; revised March 26, 2003; accepted April 7, 2003.

Disclosure: **E. Sakurai**, None; **A. Anand**, None; **B.K. Ambati**, None; **N. van Rooijen**, None; **J. Ambati**, None

The publication costs of this article were defrayed in part by page charge payment. This article must therefore be marked "*advertisement*" in accordance with 18 U.S.C. §1734 solely to indicate this fact.

Corresponding author: Jayakrishna Ambati, Department of Ophthalmology, University of Kentucky, 801 Rose Street, Lexington, KY 40536-0284; jamba2@uky.edu.

Age-related macular degeneration (AMD) is the leading cause of irreversible blindness among the elderly in most industrialized nations,[1] yet little is known about the molecular mechanisms of choroidal neovascularization (CNV), the angiogenic process responsible for most severe visual loss in patients with AMD.[2]

The presence of macrophages in histologic studies of CNV has elicited interest in their role in the development of neovascular AMD. The spatiotemporal distribution of macrophages correlates with arborizing CNV in humans[3] and in animal models.[4] In patients with AMD, macrophages are in proximity to thinned and perforated areas of Bruch's membrane[5,6] and participate in digesting the outer collagenous zone of Bruch's membrane,[6] both of which facilitate the subretinal entry of CNV.

To test directly the hypothesis that macrophages play a causal rather than coincidental role in the development of CNV, we used the technique of pharmacological macrophage depletion with liposomal clodronate (Cl_2MDP-LIP) in the laser-induced model of CNV, which captures many salient pathologic and molecular features of neovascular AMD. Although free Cl_2MDP does not penetrate cell membranes and has a short circulating half-life, Cl_2MDP-LIP is phagocytosed by macrophages and rapidly induces apoptosis[7,8] without secretion of proinflammatory cytokines by the dying macrophages.[9] Moreover, Cl_2MDP-LIP appears to have a very selective effect on macrophages and phagocytic dendritic cells. Neutrophils and lymphocytes are not directly affected by this drug.[10-12]

We sought to assess the differential contribution of macrophages in the local (submandibular) lymph nodes versus that of the circulating, splenic, and hepatic macrophages to the development of CNV in this model. We administered Cl_2MDP-LIP by intravenous (IV) injection, which leads to near complete depletion of splenic and hepatic macrophages and marginal zone dendritic cells within 24 hours, persisting for 1 to 2 weeks in mice,[10] and/or subconjunctival (SC) injection, which leads to the depletion of macrophages from the draining submandibular lymph nodes.[13]

We attempted to differentiate the contribution of circulating versus resident retinal macrophages to CNV. Cl_2MDP-LIP does not cross the blood-brain barrier (and presumably the blood-retinal barrier) until it is damaged by an inflammatory response.[14] Therefore, we administered IV Cl_2MDP-LIP before laser injury and/or after laser injury, because the latter but not the former would permit the drug access to resident macrophages in the retina. We also correlated the macrophage response to laser injury with the level of vascular endothelial growth factor (VEGF), which is operative in the development of CNV[15-21] to deduce a mechanism for the effect of macrophage depletion in this process.

METHODS

Animals

All animal experiments were in accordance with the guidelines of the University of Kentucky IACUC and ARVO Statement for the Use of

Investigative Ophthalmology & Visual Science, August 2003, Vol. 44, No. 8

Animals in Ophthalmic and Vision Research. Male wild-type C57BL/6 mice (Jackson Laboratories, Bar Harbor, ME) between 6 and 8 weeks of age were used to minimize variability, because age[22] and sex (Tanemura M, et al. *IOVS* 2001;42:ARVO Abstract 530) can influence susceptibility to CNV. For all procedures, anesthesia was achieved by intramuscular injection of 50 mg/kg ketamine HCl (Fort Dodge Animal Health, Fort Dodge, IA) and 10 mg/kg xylazine (Phoenix Scientific, St. Joseph, MO), and pupils were dilated with topical 1% tropicamide (Alcon, Fort Worth, TX).

Induction of CNV

Laser photocoagulation (532 nm, 200 mW, 100 ms, 75 m; OcuLight GL, Iridex, Mountain View, CA) was performed on both eyes of each animal on day 0 by a single individual masked to drug group assignment. Laser spots were applied in a standardized fashion around the optic nerve, using a slit lamp delivery system and a coverslip as a contact lens. The morphologic end point of the laser injury was the appearance of a cavitation bubble, a sign thought to correlate with the disruption of Bruch's membrane.

Liposomes

Clodronate (dichloromethylene diphosphonate; Cl_2MDP) was a gift of Roche Diagnostics GmbH, Mannheim, Germany. Clodronate-liposomes (Cl_2MDP-LIP) were prepared[11] as follows. In short, 86 mg phosphatidylcholine (Lipoid EPC; Lipoid, Ludwigshafen, Germany) and 8 mg cholesterol (Sigma-Aldrich, St. Louis, MO) were combined with 10 mL of a clodronate (0.7 M) solution and sonicated gently. The resultant liposomes were then washed to eliminate free drug. Empty liposomes were prepared under the same conditions with phosphate-buffered saline (PBS; Invitrogen/Gibco, Grand Island, NY) instead of the clodronate solution. Animals received 200 L Cl_2MDP-LIP or PBS-LIP through the tail vein with a 30-gauge needle on day 2 (group 1), day 0 (immediately after laser injury; group 2), day -2 and day 0 (group 3), or day 2 (group 4). At these same time points, animals received 10 L Cl_2MDP-LIP in one eye and 10 L PBS-LIP in the other injected into the subconjunctival space with a syringe (Hamilton, Reno, NV). Injections were performed in a masked fashion.

Fluorescein Angiography

Fluorescein angiography was performed with a camera and imaging system (TRC 50 IA camera; ImageNet 2.01 system; Topcon, Paramus, NJ) at 1 week after laser photocoagulation. The photographs were captured with a 20-D lens in contact with the fundus camera lens after intraperitoneal injection of 0.1 mL of 2.5% fluorescein sodium (Akorn, Decatur, IL). A retina specialist not involved in the laser photocoagulation or angiography evaluated the fluorescein angiograms at a single sitting in masked fashion.

Volume of CNV

One week after laser injury, eyes were enucleated and fixed with 4% paraformaldehyde for 30 minutes at 4°C. Eye cups obtained by removing anterior segments were washed three times in PBS, followed by dehydration and rehydration through a methanol series. After blocking twice with buffer (PBS containing 1% bovine serum albumin (BSA; Sigma-Aldrich) and 0.5% Triton X-100 (Sigma-Aldrich) for 30 minutes at room temperature, eye cups were incubated overnight at 4°C with 0.5% FITC-isolectin B4 (Vector Laboratories, Burlingame, CA), which binds to terminal -D-galactose residues on the surface of endothelial cells and selectively labels the murine vasculature, diluted with PBS containing 0.2% BSA and 0.1% Triton X-100. After two washings with PBS containing 0.1% Triton X-100, the neurosensory retina was gently detached and severed from the optic nerve. Four relaxing radial incisions were made, and the remaining RPE-choroid-sclera complex was flatmounted in antifade medium (Immu-Mount Vectashield Mounting Medium; Vector Laboratories) and coverslipped.

Flatmounts were examined with a scanning laser confocal microscope (TCS SP; Leica, Heidelberg, Germany). Vessels were visualized by exciting with blue argon laser wavelength (488 nm) and capturing emission between 515 to 545 nm. A 40 oil-immersion objective was used for all imaging studies. Horizontal optical sections (1 m step) were obtained from the surface of the RPE-choroid-sclera complex. The deepest focal plane in which the surrounding choroidal vascular network connecting to the lesion could be identified was judged to be the floor of the lesion. Any vessel in the laser treated area and superficial to this reference plane was judged as CNV. Images of each section were digitally stored. The area of CNV-related fluorescence was measured by computerized image analysis with the microscope software (TCS SP; Leica). The summation of whole fluorescent area in each horizontal section was used as an index for the volume of CNV. Imaging was performed by an operator masked to treatment group assignment.

Immunostaining

At various times during the first week after laser injury, animals were injected with 1 mL FITC-isolectin B4 through the tail vein, and retinal-RPE-choroid-scleral or RPE-choroid-scleral flatmounts were prepared 30 minutes later. These were stained with antibodies against F4/80 (5 g/mL; Serotec, Oxford, UK), expressed by retinal microglia and all mouse macrophages save those in lymphoid organs[23] or leukocyte common antigen CD45.2 (5 g/mL; eBioscience, San Diego, CA), which also identifies retinal microglia.[24] Flatmounts were examined by scanning laser confocal microscopy. An optical density plot of the selected area was generated by a histogram graphing tool in the image-analysis software (Photoshop, ver. 6.0; Adobe Systems, Mountain View, CA) to obtain a quantitative index of macrophage numbers, as described previously.[25,26] Image analysis was performed by an operator masked to treatment group assignment.

VEGF ELISA

At 3 days after injury by 12 laser spots, the RPE-choroid complex was sonicated in lysis buffer (20 mM imidazole HCl, 10 mM KCl, 1 mM $MgCl_2$, 10 mM EGTA, 1% Triton X-100, 10 mM NaF, 1 mM Na molybdate, and 1 mM EDTA with protease inhibitor; Sigma-Aldrich) on ice for 15 minutes. VEGF protein levels in the supernatant were determined by an ELISA kit (threshold of detection 3 pg/mL; R&D Systems, Minneapolis, MN) that recognizes all splice variants, at 450 to 570 nm (Emax; Molecular Devices, Sunnyvale, CA), and normalized to total protein (Bio-Rad, Hercules, CA). Duplicate measurements were performed in a masked fashion by an operator not involved in photocoagulation, imaging, or fluorescein angiography.

Statistics

Volume of CNV. The dependent variable in the analysis was the average lesion volume per eye per mouse. A linear mixed model for a split plot design was constructed with two whole plot (between mice) factors. These are treatments (i.e., timing of the treatments relative to the laser injury) and intravenous (IV) administration (Cl_2MDP-LIP or PBS-LIP). The split plot (within mice) factor was subcutaneous (SC) administration (Cl_2MDP-LIP or PBS-LIP). Post hoc comparison of means consisted of either a pair-wise comparison of means or a contrast among the means constructed with error terms, depending on whether the contrast was between or within mice, respectively. Because the variability among mice treated with IV Cl_2MDP-LIP differed substantially from the variability among mice treated with IV PBS-LIP, the linear mixed model contained different variance components for these groups. Statistical significance was determined at the 0.05 level.

F4/80 and VEGF. Quantitative immunostaining and VEGF protein data were analyzed by ANOVA with the Dunnett multiple comparison test. Results were considered significant at P 0.05.

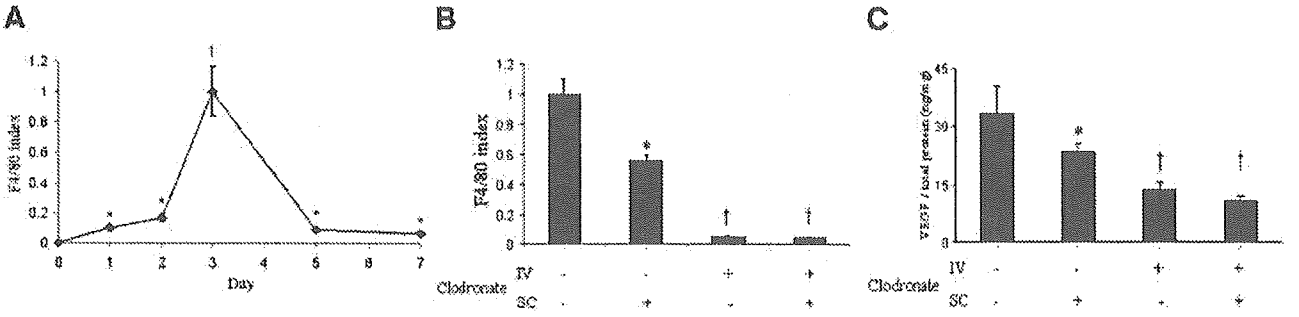

FIGURE 1. Cl_2MDP-LIP inhibited macrophage recruitment and VEGF protein expression after laser injury. (A) F4/80-positive macrophages were detected in the RPE-choroid of laser lesions within 1 day after laser injury and peaked in number at day 3. The index was normalized to peak response. *P 0.01 and †P 0.001 compared with day 0. (B) IV Cl_2MDP-LIP nearly abolished the peak macrophage response at day 3 in the RPE-choroid of laser lesions. SC Cl_2MDP-LIP partially inhibited macrophage recruitment when combined with IV PBS-LIP treatment but conferred no benefit when added to IV Cl_2MDP-LIP. *P 0.01 and †P 0.001 compared with no Cl_2MDP-LIP (PBS-LIP) treatment. (C) VEGF protein expression peaked at day 3 (data not shown). IV Cl_2MDP-LIP inhibited the VEGF protein expression response at day 3 in the RPE-choroid of laser lesions. SC Cl_2MDP-LIP partially inhibited VEGF levels when combined with IV PBS treatment but confered no benefit when added to IV Cl_2MDP-LIP. Data are expressed as the mean SEM. *P 0.01 and †P 0.001 compared with no Cl_2MDP-LIP (PBS-LIP) treatment. n 5 per group.

RESULTS

Macrophages invaded the site of laser injury within 1 day, with a peak response at 3 days, followed by rapid disappearance by 5 to 7 days (Fig. 1A). IV Cl_2MDP-LIP administration nearly abolished macrophage recruitment, whereas SC Cl_2MDP-LIP blunted the macrophage response when administered with IV PBS-LIP, but did not confer added benefit to IV Cl_2MDP-LIP (Fig. 1B). The peak macrophage number paralleled the maximal amount of VEGF protein detected in the laser lesion at 3 days (r^2 0.988; Fig. 1C) and the volume of CNV at 7 days (r^2 0.986).

Confocal planar analysis revealed marked spatial colocalization of macrophages and endothelial cells at the site of laser injury (Fig. 2). In addition, IV Cl_2MDP-LIP, and SC Cl_2MDP-LIP to a lesser extent, decreased both the peak number of macrophages and endothelial cell coverage in parallel. We also observed that, whereas macrophages were found in areas without endothelial cells, the converse was rarely the case, supporting the notion that temporally macrophages precede and promote endothelial cell proliferation. During the first 3 days after laser injury, macrophages were concentrated in the choroidal base and central substance of the CNV lesion, but were sparse near its retinal apex (Fig. 3). Also, there was no difference in the density of macrophages and retinal microglia in the retina adjacent to the laser scar compared with the remainder of the retina, using either F4/80 (Fig. 3C) or CD45.2 (similar data not shown).

The stereotypical CNV response to laser injury was markedly inhibited by IV Cl_2MDP-LIP and to a lesser extent by SC Cl_2MDP-LIP (Fig. 4). Combined IV and SC Cl_2MDP-LIP treatment 2 days before laser injury decreased CNV volume by 90.8% 3.1% (P 0.0001), immediately after laser injury by 79.2% 11.1% (P 0.0001), and before and immediately after laser injury by 91.7% 4.7% (P 0.0001), compared with combined IV and SC PBS-LIP treatment (Fig. 5). However, when IV and SC Cl_2MDP-LIP were administered 2 days after laser injury CNV volume was not significantly reduced (P 0.11). IV Cl_2MDP-LIP treatment reduced CNV volumes in eyes treated with SC Cl_2MDP-LIP or SC PBS-LIP. When coadministered with IV PBS-LIP, SC Cl_2MDP-LIP treatment 2 days before laser injury decreased CNV volumes by 24.5% 7.2% (P 0.05), immediately after laser injury by 27.8% 8.2% (P 0.05), and before and immediately after laser injury by 35.5% 7.9% (P 0.007), compared with SC PBS-LIP; however, SC Cl_2MDP-LIP did not augment the antiangiogenic effect of IV Cl_2MDP-LIP.

Pair-wise comparison of the different groups (timing of administration) revealed that IV Cl_2MDP-LIP was more effective when administered 2 days before laser injury than immediately after (P 0.05) or 2 days after (P 0.0001; Fig. 5E). Administering IV Cl_2MDP-LIP immediately after laser injury did not provide added benefit when it was administered 2 days before as well (P 0.83). When SC Cl_2MDP-LIP was combined with IV Cl_2MDP-LIP, drug treatment 2 days before was no more effective than immediately after (P 0.20), but both were more effective than 2 days after (P 0.0001).

At 1 week after laser photocoagulation, fewer lesions in Cl_2MDP-treated animals exhibited fluorescein leakage (Fig. 6). Greater suppression of angiographic leakage was found when Cl_2MDP-LIP was administered both before and immediately after laser injury.

DISCUSSION

To our knowledge, this study is the first to demonstrate that macrophage depletion by Cl_2MDP-LIP inhibits the development of laser-induced CNV, validating our hypothesis that macrophages play a pivotal role in this process. Cl_2MDP-LIP decreased the peak macrophage response in parallel with VEGF protein levels and total CNV volume. Cl_2MDP-LIP administered before and/or immediately after laser injury inhibited CNV, whereas it did not exhibit any effect when administered 2 days after laser injury. This is presumably because macrophage depletion occurs roughly 24 hours after Cl_2MDP-LIP exposure, by which time the peak macrophage response at the site of laser injury has occurred. These data show that macrophages, which previous histopathological studies of experimental and clinical CNV have shown to be closely associated with new vessels, play a causal not a coincidental role in the development of laser-induced CNV.

IV Cl_2MDP-LIP–induced inhibition of CNV was not augmented by SC Cl_2MDP-LIP, whereas the latter was observed to inhibit CNV partially when coadministered with IV PBS-LIP. The total volume of SC Cl_2MDP-LIP administered to any single animal did not exceed 20 L, which is insufficient to deplete splenic or hepatic macrophages.[13] In a model of experimental autoimmune pigment-epithelial uveitis (EAPU), IV Cl_2MDP-LIP, but not SC Cl_2MDP-LIP, inhibited EAPU,[27] suggesting that SC

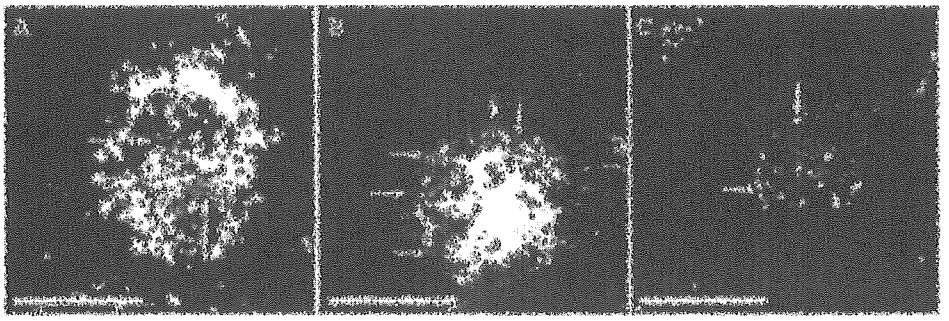

FIGURE 2. Macrophages recruited after laser injury colocalized with endothelial cells, and both responses were inhibited by Cl_2MDP-LIP. (A) Three days after laser injury in an animal treated with IV PBS-LIP, macrophages (*arrows*) stained by Cy5-F4/80 (*blue*) colocalized (*arrowheads*) with endothelial cells stained by FITC-Isolectin B4 (*green*). Colocalization by merging yielded a *cyan* color. (B) SC Cl_2MDP-LIP partially inhibited the number of macrophages (*arrows*) and CNV volume. (C) IV Cl_2MDP-LIP nearly abolished macrophage (*arrows*) and CNV response. The 1- m sections with the greatest density of F4/80 staining within laser scars are shown. Scale bar, 50 m.

FIGURE 3. Macrophages in CNV were not recruited from the resident retinal population. (A) Three days after laser injury, numerous macrophages (*arrow*) stained by Cy5-F4/80 (*blue*) were present near the choroidal base of the CNV lesion (endothelial cells stained by FITC-Isolectin B4 appear *green*). (B) The highest density of macrophages (*arrow*), many of which colocalized with endothelial cells ( ) (merge yields *cyan* color; *arrowheads*) was present in the middle of the CNV lesion. (C) A paucity of macrophages were found at the retinal surface of the CNV lesion (perimeter outlined in *white*) and in the adjacent retina (R). One-micrometer-thick sections are shown. Scale bar, 50 m.

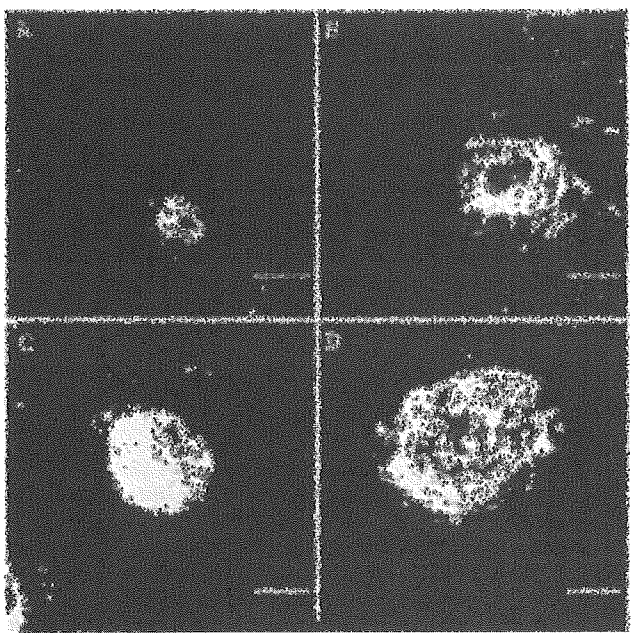

FIGURE 4. Cl_2MDP-LIP inhibited CNV 1 week after laser injury. IV Cl_2MDP-LIP administered 2 days before and immediately after laser injury suppressed CNV volume (A) to a greater degree than when administered 2 days after laser injury (B). SC Cl_2MDP-LIP administered 2 days before and immediately after laser injury in the presence of IV PBS-LIP partially inhibited CNV volume (C) compared with IV and SC PBS-LIP treatments at the same times (D). Stacked confocal images (1 m sections) of FITC-isolectin B4 labeled tissue within laser scars are shown. Scale bar, 100 m.

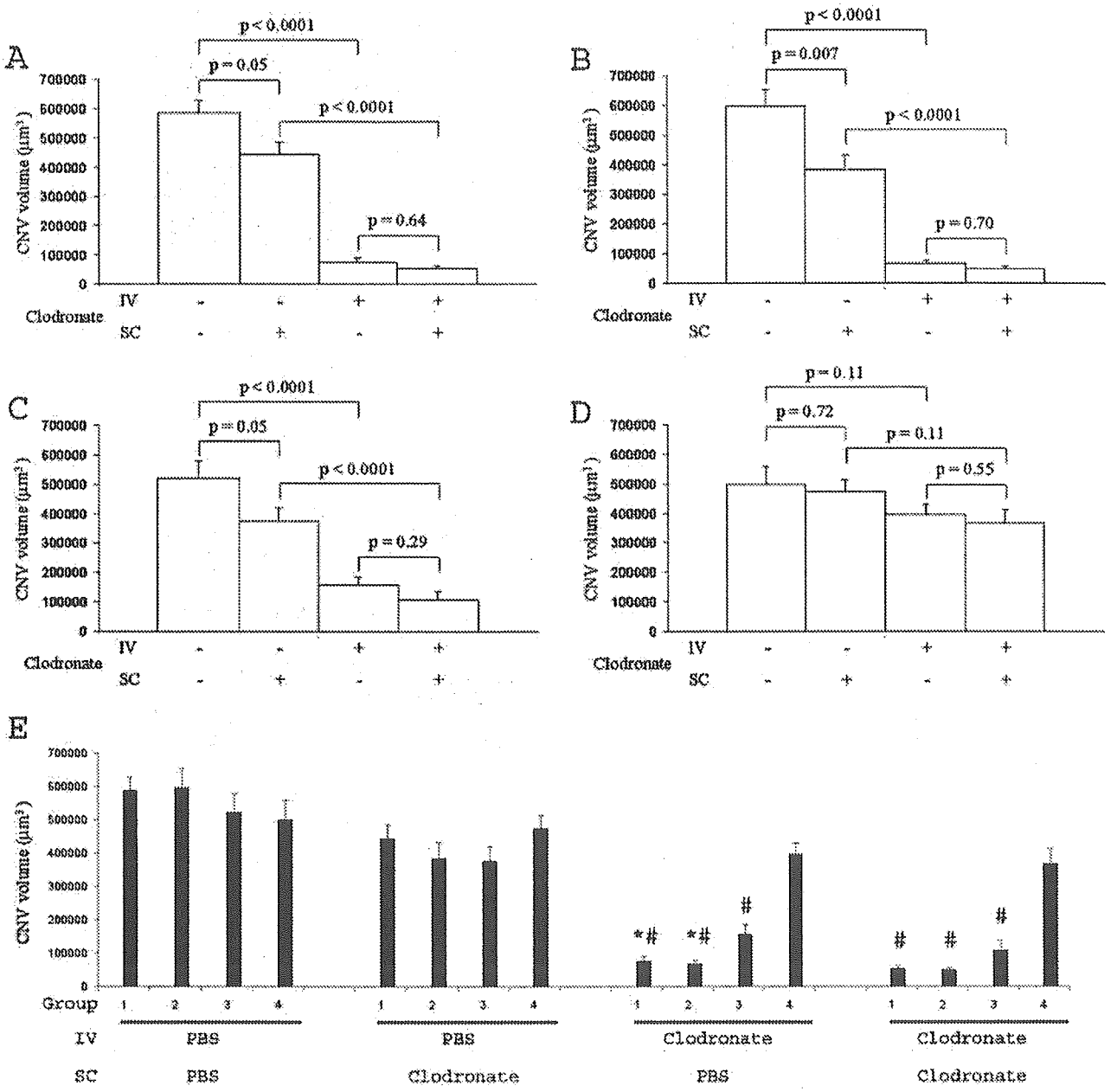

FIGURE 5. CNV volume was markedly diminished in Cl_2MDP-LIP–treated mice 1 week after laser injury. Cl_2MDP-LIP administered 2 days before laser injury (A), 2 days before and immediately after laser injury (B), and immediately after laser injury (C) demonstrated potent inhibition of CNV volume when Cl_2MDP-LIP was administered IV and mild inhibition when it was administered SC. SC Cl_2MDP-LIP did not provide added inhibition when administered with IV Cl_2MDP-LIP, but provided moderate inhibition when coadministered with IV PBS-LIP. Neither route of administration provided significant inhibition when administered 2 days after laser injury (D). (E) Pair-wise comparison of CNV volumes between group 1 (treatment 2 days before), group 2 (2 days before and immediately after), group 3 (immediately after), and group 4 (2 days after) are presented. IV Cl_2MDP-LIP was more effective when administered 2 days before laser injury (group 1 or 2) than immediately after (group 3) or 2 days after (group 4). When SC Cl_2MDP-LIP was combined with IV Cl_2MDP-LIP, drug treatments 2 days before (group 1 or 2) or immediately after (group 3) were more effective than at 2 days after (group 4). Administering IV Cl_2MDP-LIP immediately after laser injury did not provide added benefit when it was administered 2 days before, as well (group 1 versus group 2). *P 0.05 versus group 3, #P 0.0001 versus group 4. All other differences NS. n 5 for all groups.

delivery of liposomes does not exert a systemic effect. Therefore, the observed beneficial effect of SC Cl_2MDP-LIP on CNV may be attributed to depletion of regional lymph node macrophages. In aggregate, these observations suggest that the predominant pool of macrophages that infiltrate areas of laser-induced CNV is derived from the systemic circulation, although submandibular nodes make a minor contribution.

The origin of macrophages observed after laser injury has been the subject of much inquiry.[4,28–30] We found that administering IV Cl_2MDP-LIP immediately after laser injury, which provides access to resident macrophages, did not augment the inhibition of CNV induced by IV Cl_2MDP-LIP 2 days before injury. We also found no infiltration of macrophages and microglia in the retina adjacent to the laser scar. Our data provide

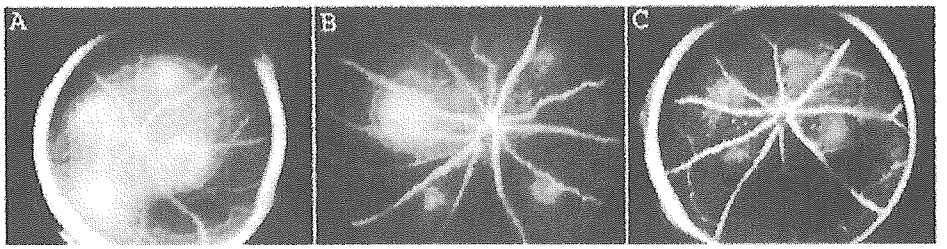

FIGURE 6. Cl_2MDP-LIP decreased angiographic leakage of laser-induced CNV. Representative late phase (6–8 minutes) fluorescein angiograms 1 week after laser injury of mice treated with IV PBS-LIP before and immediately after (A), with IV Cl_2MDP-LIP 2 days before (B), and with IV Cl_2MDP-LIP 2 days before and immediately after (C) laser injury.

direct anatomic and functional evidence that circulating rather than resident macrophages are the primary culprit in laser-induced CNV. This is consistent with the in vitro finding of polarized secretion of macrophage chemoattractant protein (MCP)-1 from the RPE into the choroid rather than the retina[31] and the in vivo finding of MCP-1 in RPE and choroid, but not in the retina, of eyes with AMD.[32]

A consensus has yet to emerge in quantifying experimental CNV: Both anatomic and functional metrics have been used. The former include measuring thickness and area on serial sections or volumes by confocal microscopy on RPE-choroidal flatmounts, aided by an endothelial cell marker. En masse volumetric measurements are less susceptible to nonorthogonality and loss or poor quality of sections than serial sectioning. Fluorescein angiography, which correlates with visual acuity in patients with AMD[33–35] and also permits longitudinal evaluation of the evolution of the laser lesions unlike histopathological examination, reflects on the leakage of these lesions, which presumably correlates with their activity. We used both anatomic and functional metrics of measuring CNV to corroborate our findings: Cl_2MDP-LIP inhibited both the anatomic volume and the angiographic leakage of laser-induced CNV.

We have shown that the leukocyte adhesion molecules CD18 and intercellular adhesion molecule (ICAM)-1 play a key role in laser-induced CNV.[36] Because liposomes do not interfere with leukocyte adhesion[37] or rolling[38] and PBS-LIP did not inhibit CNV, the antiangiogenic effects of Cl_2MDP-LIP can be attributed to depletion of macrophages alone. We infer therefore that the paracrine signals produced by macrophages promote the development of CNV. A likely signaling candidate is VEGF, as its levels were suppressed by Cl_2MDP-LIP in tandem with the number of macrophages, particularly because VEGF has been shown to be operative in CNV.[15–21]

We postulate that Cl_2MDP-LIP aborted the early-phase response to laser injury, mediated by macrophage migration, perhaps in response to overexpression of MCP-1, a stereotyped wounding response[39] that also occurs in RPE cells of AMD eyes (Spandau U, et al. *IOVS* 2000;41:ARVO Abstract 4440).[32] In support of this hypothesis, we have demonstrated that genetic ablation of MCP-1 or its cognate receptor CCR2 markedly inhibits laser-induced CNV (data not shown). However, the inhibition of CNV volume in MCP-1– or CCR2-deficient mice (75%) did not match the near abolition induced by maximal Cl_2MDP-LIP treatment, probably due to depletion by Cl_2MDP-LIP of macrophages responsive not only to MCP-1 but to other chemokines, such as macrophage inflammatory proteins-1 and - , that may play minor roles in recruiting macrophages.

Administering Cl_2MDP-LIP before or immediately after injury sharply reduced the number of macrophages in the site of laser injury, preventing the paracrine effects of these cells on endothelial cell migration and proliferation. VEGF, a major product of activated macrophages was reduced in parallel with the decrease in the number of macrophages. Laser photocoagulation leads to VEGF production by RPE cells,[40] predominantly on the choroidal side,[41] which itself can act as a macrophage chemoattractant.[42,43] However, because VEGF was reduced by Cl_2MDP-LIP, it seems that macrophages contribute perhaps more toward upregulation of VEGF than RPE or that RPE secretion of VEGF may be induced, in part, by macrophage–RPE interaction. Through their own VEGF release[44] macrophages can amplify the local VEGF response. Also macrophage-derived cytokines can stimulate VEGF production in RPE cells[45] and choroidal fibroblasts.[46] Macrophages can perpetuate their ingress by stimulating RPE cells to secrete MCP-1 into the choroid in a polarized gradient.[31] In addition to VEGF, macrophages also may produce matrix metalloproteinases (MMPs) directly[47] or through VEGF, which induces MMP expression in endothelial cells,[48] These MMPs, which have been found in CNV in AMD,[49] can facilitate endothelial cell migration during angiogenesis.

These findings may have some relevance to CNV in AMD, for although the laser injury model may involve processes not relevant to AMD, it captures many of the important features of the human condition. Laser photocoagulation that disrupts Bruch's membrane can induce CNV in humans.[50] Both in experimental models and in AMD, newly formed vessels that are functionally incompetent[51,52] project into the subretinal space through defects in Bruch's membrane. Aggregation of leukocytes near arborizing neovascular tufts[3,4,45] is another shared feature of experimental and clinical CNV. Immunostaining has demonstrated the presence of VEGF and its receptors,[40,53] basic fibroblast growth factor,[54,55] transforming growth factor- ,[54,56] tumor necrosis factor- ,[45] Fas, and Fas-ligand[57,58] in cells of the CNV membranes in both conditions.

Because angiogenesis is a complex process with multiple redundant and intertwined cascades, it is remarkable that macrophage depletion alone nearly abolished CNV. This suggests, at least in this model of CNV, that macrophages and cytokines derived from them are requisite in this process and buttresses the growing body of evidence implicating leukocytes in the initiation of angiogenesis. Although macrophage inactivation could lead to immunosuppression, no overt infection was observed in our study involving transient macrophage depletion or by other investigators.[9,11] Although the clinical implications of transient, partial depletion of macrophages with Cl_2MDP-LIP will be apparent only in human trials, MCP-1 or CCR2 may be attractive molecular targets, particularly with local drug delivery.[59]

Acknowledgments

The authors thank Robinette King and Guojin Chen for technical assistance; Richard J. Kryscio, University of Kentucky Biostatistics Consulting Unit, for statistical analyses; and Ambati M. Rao, Delwood C. Collins, and P. Andrew Pearson for ongoing support.

References

1. Smith W, Assink J, Klein R, et al. Risk factors for age-related macular degeneration: pooled findings from three continents. *Ophthalmology.* 2001;108:697–704.
2. Macular Photocoagulation Study Group. Argon laser photocoagulation for neovascular maculopathy: five-year results from randomized clinical trials. *Arch Ophthalmol.* 1991;109:1109–1114.

3. Grossniklaus HE, Cingle KA, Yoon YD, Ketkar N, L'Hernault N, Brown S. Correlation of histologic 2-dimensional reconstruction and confocal scanning laser microscopic imaging of choroidal neovascularization in eyes with age-related maculopathy. *Arch Ophthalmol.* 2000;118:625–629.
4. Nishimura T, Goodnight R, Prendergast RA, Ryan SJ. Activated macrophages in experimental subretinal neovascularization. *Ophthalmologica.* 1990;200:39–44.
5. Killingsworth MC, Sarks JP, Sarks SH. Macrophages related to Bruch's membrane in age-related macular degeneration. *Eye.* 1990; 4:613–621.
6. van der Schaft TL, Mooy CM, de Bruijn WC, de Jong PT. Early stages of age-related macular degeneration: an immunofluorescence and electron microscopy study. *Br J Ophthalmol.* 1993;77: 657–661.
7. Naito M, Nagai H, Kawano S, et al. Liposome-encapsulated dichloromethylene diphosphonate induces macrophage apoptosis in vivo and in vitro. *J Leukoc Biol.* 1996;60:337–344.
8. van Rooijen N, Sanders A, van den Berg TK. Apoptosis of macrophages induced by liposome-mediated intracellular delivery of clodronate and propamidine. *J Immunol Methods.* 1996;193: 93–99.
9. van Rooijen N, Sanders A. Elimination, blocking, and activation of macrophages: three of a kind? *J Leukoc Biol.* 1997;62:702–709.
10. van Rooijen N, Kors N, Kraal G. Macrophage subset repopulation in the spleen: differential kinetics after liposome-mediated elimination. *J Leukoc Biol.* 1989;45:97–104.
11. Van Rooijen N, Sanders A. Liposome mediated depletion of macrophages: mechanism of action, preparation of liposomes and applications. *J Immunol Methods.* 1994;174:83–93.
12. Alves-Rosa F, Stanganelli C, Cabrera J, van Rooijen N, Palermo MS, Isturiz MA. Treatment with liposome-encapsulated clodronate as a new strategic approach in the management of immune thrombocytopenic purpura in a mouse model. *Blood.* 2000;96:2834–2840.
13. Van der Veen G, Broersma L, Van Rooijen N, Van Rij G, Van der Gaag R. Cytotoxic T lymphocytes and antibodies after orthotropic penetrating keratoplasty in rats treated with dichloromethylene diphosphonate encapsulated liposomes. *Curr Eye Res.* 1998;17: 1018–1026.
14. Huitinga I, Damoiseaux JG, van Rooijen N, Dopp EA, Dijkstra CD. Liposome mediated affection of monocytes. *Immunobiology.* 1992;185:11–19.
15. Cui JZ, Kimura H, Spee C, Thumann G, Hinton DR, Ryan SJ. Natural history of choroidal neovascularization induced by vascular endothelial growth factor in the primate. *Graefes Arch Clin Exp Ophthalmol.* 2000;238:326–333.
16. Spilsbury K, Garrett KL, Shen WY, Constable IJ, Rakoczy PE. Overexpression of vascular endothelial growth factor (VEGF) in the retinal pigment epithelium leads to the development of choroidal neovascularization. *Am J Pathol.* 2000;157:135–144.
17. Schwesinger C, Yee C, Rohan RM, et al. Intrachoroidal neovascularization in transgenic mice overexpressing vascular endothelial growth factor in the retinal pigment epithelium. *Am J Pathol.* 2001;158:1161–1172.
18. Baffi J, Byrnes G, Chan CC, Csaky KG. Choroidal neovascularization in the rat induced by adenovirus mediated expression of vascular endothelial growth factor. *Invest Ophthalmol Vis Sci.* 2000;41:3582–3589.
19. Honda M, Sakamoto T, Ishibashi T, Inomata H, Ueno H. Experimental subretinal neovascularization is inhibited by adenovirus-mediated soluble VEGF/flt-1 receptor gene transfection: a role of VEGF and possible treatment for SRN in age-related macular degeneration. *Gene Ther.* 2000;7:978–985.
20. Kwak N, Okamoto N, Wood JM, Campochiaro PA. VEGF is major stimulator in model of choroidal neovascularization. *Invest Ophthalmol Vis Sci.* 2000;41:3158–3164.
21. Krzystolik MG, Afshari MA, Adamis AP, et al. Prevention of experimental choroidal neovascularization with intravitreal anti-vascular endothelial growth factor antibody fragment. *Arch Ophthalmol.* 2002;120:338–346.
22. Espinosa-Heidmann DG, Suner I, Hernandez EP, Frazier WD, Csaky KG, Cousins SW. Age as an independent risk factor for severity of experimental choroidal neovascularization. *Invest Ophthalmol Vis Sci.* 2002;43:1567–1573.
23. Austyn JM, Gordon S. F4/80, a monoclonal antibody directed specifically against the mouse macrophage. *Eur J Immunol.* 1981; 11:805–815.
24. Chen L, Yang P, Kijlstra A. Distribution, markers, and functions of retinal microglia. *Ocul Immunol Inflamm.* 2002;10:27–39.
25. Lehr HA, van der Loos CM, Teeling P, Gown AM. Complete chromogen separation and analysis in double immunohistochemical stains using Photoshop-based image analysis. *J Histochem Cytochem.* 1999;47:119–126.
26. Lehr HA, Mankoff DA, Corwin D, Santeusanio G, Gown AM. Application of Photoshop-based image analysis to quantification of hormone receptor expression in breast cancer. *J Histochem Cytochem.* 1997;45:1559–1565.
27. Broekhuyse RM, Huitinga I, Kuhlmann ED, Rooijen NV, Winkens HJ. Differential effect of macrophage depletion on two forms of experimental uveitis evoked by pigment epithelial membrane protein (EAPU), and by melanin-protein (EMIU). *Exp Eye Res.* 1997; 65:841–848.
28. Gloor BP. On the question of the origin of macrophages in the retina and the vitreous following photocoagulation (autoradiographic investigations by means of 3H-thymidine). *Albrecht Von Graefes Arch Klin Exp Ophthalmol.* 1974;190:183–194.
29. Ishikawa Y, Momoeda S, Yoshitomi F. Origin of macrophage in photocoagulated rabbit retina. *Jpn J Ophthalmol.* 1983;27:138–148.
30. Tso MO. Photic maculopathy in rhesus monkey: a light and electron microscopic study. *Invest Ophthalmol.* 1973;12:17–34.
31. Holtkamp GM, De Vos AF, Peek R, Kijlsta A. Analysis of the secretion pattern of monocyte chemotactic protein-1 (MCP-1) and transforming growth factor-beta 2 (TGF-beta2) by human retinal pigment epithelial cells. *Clin Exp Immunol.* 1999;118:35–40.
32. Grossniklaus HE, Ling JX, Wallace TM, et al. Macrophage and retinal pigment epithelium expression of angiogenic cytokines in choroidal neovascularization. *Mol Vis.* 2002;8:119–126.
33. Miller JW, Schmidt-Erfurth U, Sickenberg M, et al. Photodynamic therapy with verteporfin for choroidal neovascularization caused by age-related macular degeneration: results of a single treatment in a phase 1 and 2 study. *Arch Ophthalmol.* 1999;117:1161–1173.
34. Treatment of Age Related Macular Degeneration with Photodynamic Therapy (TAP) Study Group. Photodynamic therapy of subfoveal choroidal neovascularization in age-related macular degeneration with verteporfin: one-year results of 2 randomized clinical trials: TAP report. *Arch Ophthalmol.* 1999;117:1329–1345.
35. Treatment of Age Related Macular Degeneration with Photodynamic Therapy (TAP) Study Group. Photodynamic therapy of subfoveal choroidal neovascularization in age-related macular degeneration with verteporfin: two-year results of 2 randomized clinical trials: TAP Report 2. *Arch Ophthalmol.* 2001;119:198–207.
36. Sakurai E, Taguchi H, Anand A, et al. Targeted disruption of the CD18 or ICAM-1 gene inhibits choroidal neovascularization. *Invest Ophthalmol Vis Sci.* 2003;44:2743–2749.
37. Baatz H, Puchta J, Reszka R, Pleyer U. Macrophage depletion prevents leukocyte adhesion and disease induction in experimental melanin-protein induced uveitis. *Exp Eye Res.* 2001;73:101–109.
38. Malhotra R, Taylor NR, Bird MI. Anionic phospholipids bind to L-selectin (but not E-selectin) at a site distinct from the carbohydrate-binding site. *Biochem J.* 1996;314:297–303.
39. DiPietro LA, Polverini PJ, Rahbe SM, Kovacs EJ. Modulation of JE/MCP-1 expression in dermal wound repair. *Am J Pathol.* 1995; 146:868–875.
40. Wada M, Ogata N, Otsuji T, Uyama M. Expression of vascular endothelial growth factor and its receptor (KDR/flk-1) mRNA in experimental choroidal neovascularization. *Curr Eye Res.* 1999; 18:203–213.
41. Blaauwgeers HG, Holtkamp GM, Rutten H, et al. Polarized vascular endothelial growth factor secretion by human retinal pigment epithelium and localization of vascular endothelial growth factor receptors on the inner choriocapillaris: evidence for a trophic paracrine relation. *Am J Pathol.* 1999;155:421–428.

42. Clauss M, Weich H, Breier G, et al. The vascular endothelial growth factor receptor Flt-1 mediates biological activities: implications for a functional role of placenta growth factor in monocyte activation and chemotaxis. *J Biol Chem.* 1996;271:17629-17634.
43. Barleon B, Sozzani S, Zhou D, Weich HA, Mantovani A, Marme D. Migration of human monocytes in response to vascular endothelial growth factor (VEGF) is mediated via the VEGF receptor flt-1. *Blood.* 1996;87:3336-3343.
44. Harmey JH, Dimitriadis E, Kay E, Redmond HP, Bouchier-Hayes D. Regulation of macrophage production of vascular endothelial growth factor (VEGF) by hypoxia and transforming growth factor beta-1. *Ann Surg Oncol.* 1998;5:271-278.
45. Oh H, Takagi H, Takagi C, et al. The potential angiogenic role of macrophages in the formation of choroidal neovascular membranes. *Invest Ophthalmol Vis Sci.* 1999;40:1891-1898.
46. Kvanta A. Expression and regulation of vascular endothelial growth factor in choroidal fibroblasts. *Curr Eye Res.* 1995;14: 1015-1020.
47. Banda MJ, Werb Z. Mouse macrophage elastase: purification and characterization as a metalloproteinase. *Biochem J.* 1981;193: 589-605.
48. Lamoreaux WJ, Fitzgerald ME, Reiner A, Hasty KA, Charles ST. Vascular endothelial growth factor increases release of gelatinase A and decreases release of tissue inhibitor of metalloproteinases by microvascular endothelial cells in vitro. *Microvasc Res.* 1998;55: 29-42.
49. Steen B, Sejersen S, Berglin L, Seregard S, Kvanta A. Matrix metalloproteinases and metalloproteinase inhibitors in choroidal neovascular membranes. *Invest Ophthalmol Vis Sci.* 1998;39:2194-2200.
50. Francois J, De Laey JJ, Cambie E, Hanssens M, Victoria-Troncoso V. Neovascularization after argon laser photocoagulation of macular lesions. *Am J Ophthalmol.* 1975;79:206-210.
51. Tobe T, Ortega S, Luna JD, et al. Targeted disruption of the FGF2 gene does not prevent choroidal neovascularization in a murine model. *Am J Pathol.* 1998;153:1641-1646.
52. Sarks SH, Van Driel D, Maxwell L, Killingsworth M. Softening of drusen and subretinal neovascularization. *Trans Ophthalmol Soc UK.* 1980;100:414-422.
53. Otani A, Takagi H, Oh H, et al. Vascular endothelial growth factor family and receptor expression in human choroidal neovascular membranes. *Microvasc Res.* 2002;64:162-169.
54. Amin R, Puklin JE, Frank RN. Growth factor localization in choroidal neovascular membranes of age-related macular degeneration. *Invest Ophthalmol Vis Sci.* 1994;35:3178-3188.
55. Ogata N, Matsushima M, Takada Y, et al. Expression of basic fibroblast growth factor mRNA in developing choroidal neovascularization. *Curr Eye Res.* 1996;15:1008-1018.
56. Ogata N, Yamamoto C, Miyashiro M, Yamada H, Matsushima M, Uyama M. Expression of transforming growth factor- mRNA in experimental choroidal neovascularization. *Curr Eye Res.* 1997; 16:9-18.
57. Hinton DR, He S, Lopez PF. Apoptosis in surgically excised choroidal neovascular membranes in age-related macular degeneration. *Arch Ophthalmol.* 1998;116:203-209.
58. Kaplan HJ, Leibole MA, Tezel T, Ferguson TA. Fas ligand (CD95 ligand) controls angiogenesis beneath the retina. *Nat Med.* 1999; 5:292-297.
59. Ambati J, Gragoudas ES, Miller JW, et al. Transscleral delivery of bioactive protein to the choroid and retina. *Invest Ophthalmol Vis Sci.* 2000;41:1186-1191.

45. リポフスチン構成成分 A2e の網膜色素上皮細胞および脈絡膜新生血管に及ぼす影響

入山　彩、高橋秀徳、井上裕治、柳　靖雄、玉置泰裕
(東京大)

研究要旨　網膜色素上皮(RPE)へのリポフスチンの沈着は滲出型加齢黄斑変性症(AMD)の前駆病変と考えられている。リポフスチンの構成成分の一つである A2E が蓄積することにより RPE に障害を与えることはいままでの研究より明らかにされている。しかし A2E が生体内でどのような生理活性を持つかは明らかになってない。今回我々はリポフスチンの構成成分である A2e の脈絡膜新生血管 (CNV) 発生への関与及びそのメカニズムを検討した。A2e は RPE を障害し、血管新生因子、血管抑制因子を介し CNV の発生及び伸展に関与している可能性が示された。又そのメカニズムの一因としてレチノイン酸受容体の活性化が示唆された。

A. 研究目的

網膜色素上皮(RPE)へのリポフスチンの沈着は滲出型加齢黄斑変性症(AMD)の前駆病変と考えられている。今回我々はリポフスチンの構成成分である A2e の脈絡膜新生血管 (CNV) 発生への関与及びそのメカニズムを検討した。

B. 研究方法

まずHec293細胞を用いA2eを負荷しルシフェラーゼアッセイを用い各種核内受容体に対する影響を検討した。次にヒト RPE 細胞株の ARPE19 細胞を用い A2e を負荷し RT−PCR 方を用い、レチノイン酸受容体のターゲット遺伝子である、SCD、NORPEG の発現を検討した。又、ARPE19 細胞を用い A2e を負荷し 24 時間後 VEGF, PEDF, HIF-1 の発現を ELISA, RT-PCR 法を用い検討した。

更に Brown Norway ラット網膜下に A2e を注入し (2.5×10^{-6}M、0,5μl)、3 週間後 RT-PCR 法で VEGF, HIF-1 の RPE と脈絡膜での発現を検討した。又、A2e 投与後、脈絡膜伸展標本にて、RPE への影響を形態学的に評価し、更にパラフィン切片を作成し、免疫染色法により VEGF の発現を検討した。次にレーザー誘発性 CNV をラット眼底に作成し CNV の活動性を蛍光眼底造影にて検討した。

(倫理面への配慮)

動物実験は ARVO Statement に従い行った。

C. 研究結果

ルシフェラーゼアッセイでは A2e が核内受容体のうちレチノイン酸受容体のみを活性化する事が示された。又レチノイン酸受容体のリガンドである atRA と同様に濃度依存性にレチノイン受容体を活性化し、又 A2e は atRA と相互増幅作用を認めた。 ARPE19

細胞においてA2e負荷によりatRAと同様にSCD, NORPEGの発現の上昇が認められた。ARPE19細胞においてA2e負荷によりmRNA及び蛋白レベルでVEGF, HIF-1の発現の上昇、PEDFの発現の低下が認められた(図1)。

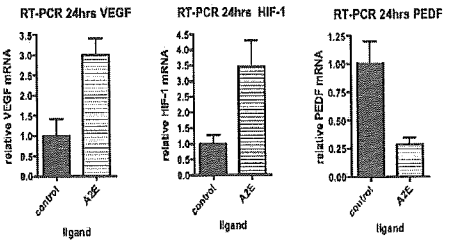

図1　A2e負荷24時間後RT-PCR

ラットではA2e網膜下注入によりRPE、脈絡膜においてVEGF, HIF-1の上昇を認め、RPE-脈絡膜伸展標本ではRPE数の減少および形態不整が認められた。(図2) 免疫染色法においてVEGFの発現の増強が認められた。

更に対照眼では低出力レーザー照射でCNVが認められなかったが、A2e投与眼では認められた。

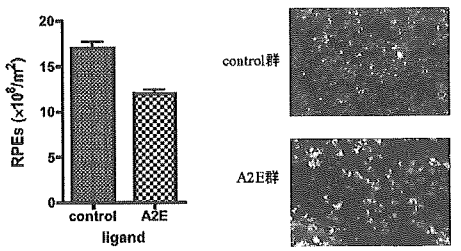

図2：A2e網膜下注入によるRPE数減少、形態変化

D. 考察

今回の研究の結果からAMDにおけるCNV発生の一因としてA2eが関与していることが示唆された。加齢により網膜色素上皮に蓄積したA2eがレチノイン酸を活性化することによりHIF-1、VEGFといった血管新生因子の発現を上昇させ、PEDFといった血管新生抑制因子の発現を低下させ、CNVを発生させ、又、PEDを障害し、伸展も促している可能性が示された。今後A2eのレチノイン酸受容体の活性化の抑制がAMDの新しい治療のターゲットとなりうる可能性が今回の研究によって示唆された

E. 結論

A2eはRPEを障害し、血管新生因子、血管新生抑制因子を介しCNVの発生及び伸展に関与している可能性が示された。又そのメカニズムの一因としてレチノイン酸受容体の活性化が示唆された。

F. 健康危険情報

なし

G. 研究発表

1. 論文発表

1. Iriyama A et al: Light-induced gene transfer forom packaged DNA enveloped in a dendrimeric photosensitizer. Nature Materials 4: 934-941, 2005.

2. 学会発表

なし

H．知的財産権の出願・登録状況

1．特許取得

なし

2．実用新案登録

なし

3．その他

なし

I．参考文献

1. Holz,F et al: Invest.Ophthalmol. Visual Sci. 40: 737-743, 1999.
2. Eldred, G. E. et al: Nature.361: 724-726, 1993.
3. Sparrow, J. et al: Invest.Ophthalmol. Visual Sci.40: 2998-2995, 1999.

Light-induced gene transfer from packaged DNA enveloped in a dendrimeric photosensitizer

NOBUHIRO NISHIYAMA[1]*, AYA IRIYAMA[2]*, WOO-DONG JANG[3], KANJIRO MIYATA[3], KEIJI ITAKA[3], YUJI INOUE[2], HIDENORI TAKAHASHI[2], YASUO YANAGI[2], YASUHIRO TAMAKI[2], HIROYUKI KOYAMA[4] AND KAZUNORI KATAOKA[1,3,5†]

[1]Center for Disease Biology and Integrative Medicine, Graduate School of Medicine, The University of Tokyo, 7-3-1 Hongo, Bunkyo-ku, Tokyo 113-0033, Japan
[2]Department of Ophthalmology, University of Tokyo Hospital, 7-3-1 Hongo, Bunkyo-ku, Tokyo 113-8655, Japan
[3]Department of Materials Engineering, Graduate School of Engineering, The University of Tokyo, 7-3-1 Hongo, Bunkyo-ku, Tokyo 113-8656, Japan
[4]Department of Clinical Vascular Regeneration, The University of Tokyo Hospital, 7-3-1 Hongo, Bunkyo-ku, Tokyo 113-8655, Japan
[5]Core Research Program for Evolutional Science and Technology (CREST) from Japan Science and Technology Agency (JST), Japan
*These authors contributed equally to this paper
†e-mail: kataoka@bmw.t.u-tokyo.ac.jp

Published online: XX Month XXXX; doi:10.1038/nmatXXXX

The control of gene transfection in the body is a core issue in gene therapy. Photochemical internalization is a technology that allows light-induced delivery of DNA, drugs or other biological factors directly inside cells. Usually it requires that a photosensitizer be added to the drug delivery system to photochemically destabilize the endosomal membrane. Here we present a system for *in vivo* DNA delivery in which these two components are assembled into one structure. This is a ternary complex composed of a core containing DNA packaged with cationic peptides and enveloped in anionic dendrimer phthalocyanine, which provides the photosensitizing action. The ternary complex showed more than 100-fold photochemical enhancement of transgene expression *in vitro* with reduced photocytotoxicity. In an animal experiment, subconjuctival injection of the ternary complex followed by laser irradiation resulted in transgene expression only in the laser-irradiated site. This work demonstrates different biomedical applications for dendrimers and success in the photochemical-internalization-mediated gene delivery *in vivo*.

There has been a strong incentive for the development of safe and effective gene vectors to achieve successful *in vivo* gene therapy[1–4]. Compared with viral vectors with an inherent risk for clinical use, non-viral synthetic vectors have received much attention owing to the advantages of safety, simplicity of use and ease of mass production[1–4]. A promising approach to the design of synthetic vectors is the use of cationic polymers and peptides. In general, the plasmid DNA (pDNA)/polycation complexes (polyplexes) are internalized by the cell through the endocytic pathway and need to be released from the endosome to deliver the genes to the nucleus. It is well known that this endosomal escape of the polyplexes is the main obstacle to obtaining efficient transfection[5]. Polycations possessing a buffering capacity, such as polyethylenimine (PEI), show a high *in vitro* transfection activity owing to the so-called proton sponge effect[5]; however, it is probable that the inherent cytotoxicity will impair their clinical utility as gene carriers. Hence, further efforts need to be devoted to the development of synthetic vectors especially for *in vivo* use.

In contrast, site-specific gene transfer to somatic cells is strongly desired; however, the existing vectors, including the viral and non-viral vectors, might have great difficulty in achieving *in vivo* transfection in a site-specific manner. In this regard, a different concept has been proposed[6–10], photochemical internalization (PCI): the cytoplasmic delivery of macromolecular compounds is enhanced by the photochemical disruption of the endosomal membrane using light and a hydrophilic photosensitizer. This smart concept is, in principle, applicable to the *in vivo* gene delivery in a light-sensitive manner[10]. However, the cytotoxicity is accompanied by photochemical reactions in the cell, and this might need to be

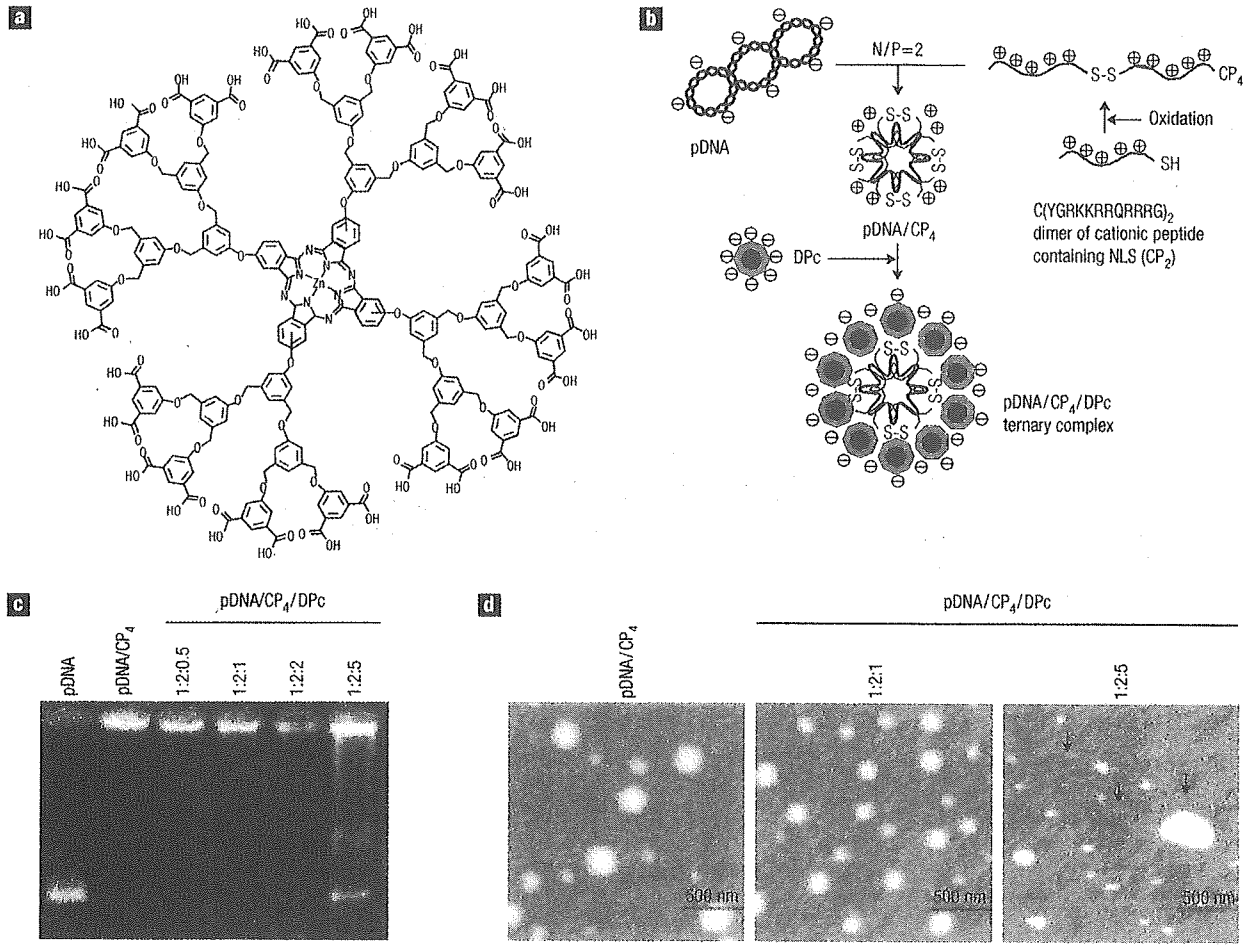

Figure 1 Preparation and characterization of the ternary complex. a, The chemical structure of ionic DPc. **b**, A scheme for preparation of the pDNA/CP_4/DPc ternary complex. **c**, Gel retardation assay of the pDNA/CP_4 polyplex prepared at an N/P ratio of 2, and the ternary complexes with varying charge molar ratios of pDNA/CP_4/DPc. **d**, AFM images of the pDNA/CP_4 and pDNA/CP_4/DPc complexes. Arrow heads indicate plasmid DNA released from the ternary complexes.

reduced before considering further applications of this technology. Moreover, there is still room for optimization and modification for *in vivo* applications. From the viewpoint of materials science, this concept can be integrated into nanodevices for drug and gene delivery.

In the present paper, we assume that the control of subcellular localization of photosensitizers maybe a key to the PCI-mediated gene delivery with reduced cytotoxicity, because the photodamage to sensitive organelles other than the endosomal membrane, for example the plasma and mitochondrial membranes, might be responsible for the photocytotoxicity[11]. In addition, gene carriers should be equipped with a photosensitizing unit as one component for *in vivo* applications. These assumptions motivated us to develop a light-responsive gene carrier based on a ternary complex of pDNA, cationic peptides and anionic dendrimer-based photosensitizers (dendrimer phthalocyanine: DPc; Fig. 1a). Dendrimers, the three-dimensional tree-like branched macromolecules, have attracted growing interest as materials for drug and gene delivery[12–16], and the ternary complex is a different biomedical application of dendrimers. The ternary complex has shown significant photochemical enhancement of the transgene expression *in vitro* with reduced photocytotoxicity and *in vivo* gene transfer to the conjunctival tissue in the rat eye in a light-selective manner.

The ternary complex is composed of a core of a pDNA/cationic polymer polyplex enveloped with anionic DPc (Fig. 1a) as illustrated in Fig. 1b. DPc possesses a centre phthalocyanine molecule surrounded by a second generation of aryl ether dendrons, and 32 carboxyl groups on the periphery of DPc allow polyion complex formation with cationic polyplexes. In the present study, the core polyplex was formed from a quadruplicated cationic peptide (CP_4), where a peptide (CP_2: C(YGRKKRRQRRRG)$_2$)) was dimerized through a disulphide linkage, and pDNA was mixed with the CP_4 peptide at a molar ratio of cationic amino acids to a phosphate anion in DNA (N/P ratio) of 2. It has been demonstrated[17] that CP_2 and CP_4 contain a nuclear localization sequence (NLS) and thereby effectively mediate the gene transfection to the cell with the aid of conventional transfection reagents such as PEI and LipofectAMINE to promote the endosomal escape of the polyplex. Thus, these potent cationic peptides were used for the formation of the ternary complex to ensure the efficient gene transfection following the endosomal escape of the polyplex.

In this study, the ternary complexes were prepared by varying the charge molar ratios of pDNA/CP_4/DPc, and the complex formation was confirmed by a gel retardation assay (Fig. 1c). As a result, pDNA was incorporated into the complexes with charge ratios up to 1:2:2, but was excluded from the complex with a charge

Table 1 Size, size distribution and ζ-potential of the electrostatic assemblies containing plasmid DNA.

	Cumulant diameter (nm)	Polydispersity index	ζ-potential (mV)
pDNA/PEI (1:10)	127.8	0.211	23.8±0.1
pDNA/CP_4 (1:2)	100.8	0.185	21.3±2.3
pDNA/CP_4/DPc (1:2:0.5)	149.7	0.115	−8.5±3.6
pDNA/CP_4/DPc (1:2:1)	130.8	0.108	−29.2±2.6
pDNA/CP_4/DPc (1:2:2)	107.7	0.143	−23.2±0.9
pDNA/CP_4/DPc (1:2:5)	267.1	0.180	−49.6±0.7
pDNA/CP_4/PAA* (1:2:0.5)	621.2	0.444	−27.1±0.8
pDNA/CP_4/PAA (1:2:1)	672.0	0.477	−25.8±0.4
pDNA/CP_4/PAA (1:2:2)	912.3	0.361	−24.3±0.8
pDNA/CP_4/PAA (1:2:5)	1426	0.278	−25.3±2.3

* PAA: Poly(aspartic acid) homopolymer with a polymerization degree of 26

ratio of 1:2:5. The release of pDNA from the 1:2:5 complex was also observed by atomic force microscopy (AFM) as shown in Fig. 1d. Thus, addition of excess DPc might disintegrate the pDNA/CP_4 polyplex. The size, polydispersity index and ζ-potential of the pDNA/CP_4/DPc ternary complexes are summarized in Table 1. The addition of DPc to the positively charged pDNA/CP_4 polyplex gave negative ζ-potential values, suggesting the formation of ternary complexes covered with anionic DPc. A decrease in the size of the ternary complexes with increasing DPc ratios may be attributed to shrinkage of the cationic peptide corona on the polyplex surface through electrostatic interaction with DPc. Surface modification with anionic DPc provided the 1:2:1 and 1:2:2 complexes with excellent colloidal stability, whereas the 1:2:0.5 complex possessing an almost neutral ζ-potential value tended to precipitate in several hours. Significantly, the ternary complexes showed much lower polydispersity indices compared with the pDNA/CP_4 or PEI polyplexes (Table 1). The AFM observation has revealed consistently that the 1:2:1 complex consists of spherical particles with a narrow size distribution, which is in marked contrast to the pDNA/CP_4 polyplex containing large aggregates (Fig. 1d). Note that the addition of poly(aspartic acid) (PAA) homopolymer with a polymerization degree of 26 to the pDNA/CP_4 polyplex resulted in a large aggregate formation (Table 1). Hence, the three-dimensional structure of DPc is assumed to play an essential role in the formation of a ternary complex with a narrow size distribution and excellent colloidal stability. The layer-by-layer assemblies of oppositely charged polyelectrolytes onto colloidal particles have attracted considerable attention[18,19]; however, the pDNA/CP_4/DPc ternary complex is definitely discriminated from the layer-by-layer assemblies, because a core composed of hard materials is not required for the formation of the ternary complex. Thus, the ternary complex presented here is a supramolecular assembly consisting of a pDNA/CP_4 polyplex core and a DPc envelope.

The properties of DPc and the ternary complex related to the initial steps in the gene transfection to the cell (that is, processes from the cellular uptake to when photodamage to the endosomal membrane occurred) were evaluated, because the ternary complex was designed to control these processes. First, the cellular uptake of the ternary complex was evaluated by flow cytometry using a fluorescein-labelled pDNA, as shown in Fig. 2a. The amount of cellular uptake of the ternary complexes was less than that of cationic polyplexes such as pDNA/CP_4 and pDNA/PEI, and decreased as the DPc ratio increased. The ternary complex covered with anionic DPc should have a lower affinity for the negatively charged plasma membrane of cells, accounting for the results in Fig. 2a.

The pH-dependent hydrophilic/hydrophobic behaviour of DPc and its possible interaction with cell membranes was estimated by octanol/water partitioning, which is a common method for evaluation of drug–membrane interactions[20]. The partitioning (%) of DPc to the octanol phase increased as the pH decreased to 5.0–5.5 (Fig. 2b), suggesting the increased hydrophobicity of DPc and possible interactions with cell membranes under low-pH conditions. Because the DPc consists of a hydrophobic dendritic framework, the protonation of the peripheral carboxyl group under acidic conditions might increase its hydrophobicity. This result suggests that DPc may be released from the ternary complex under endosomal pH conditions to interact with the endosomal membrane, while electrostatically interacting with the positively charged surface of the polyplex at physiological pH. This assumption offers an interesting opportunity to selectively photodamage the endosomal membrane for effective PCI.

Figure 2c shows the subcellular distribution of FITC-labelled dextran co-incubated with the 1:2:1 ternary complex. It was demonstrated that FITC-dextran showed diffused fluorescence throughout the cytoplasm after photoirradiation, whereas it showed punctuated fluorescence corresponding to localization in the endosome and/or lysosome before photoirradiation. This result suggests the capability of the ternary complex of releasing the contents in the vesicular organelles to the cytoplasm on photoirradiation.

To evaluate the potential of the ternary complex for PCI-mediated gene delivery, *in vitro* transfection experiments were performed on HeLa cells with a luciferase (Luc) reporter gene in the presence or absence of photoirradiation. Simultaneously, the cell viability was assessed by MTT assay (see Methods). Figure 3a shows the transfection efficiency and cytotoxicity of the pDNA/CP_4 polyplex and pDNA/CP_4/DPc ternary complexes with varying charge ratios of DPc after irradiation of the light with increasing fluence. In this experiment, the cells were photoirradiated after 6-h incubation with each complex and fresh medium replacement, followed by 48-h post-incubation. The 1:2:1 and 1:2:2 ternary complexes achieved more than 100-fold photochemical enhancement of the transgene expression with minimal photocytotoxicity over a wide range of fluence (−3.6 J cm^{-2}), whereas the 1:2:5 ternary complex, having a disordered structure, showed the lowest transfection activity (Fig. 3a). Note that a further increase in fluence resulted in a significant increase in the photocytotoxicity of the ternary complexes (a 50–70% decrease in the viability at 5.4 J cm^{-2}) (see Supplementary Information, Fig. S1). The transfection to a different cell line (that is, 293T cells) revealed similar photochemical enhancement of transgene expression by the ternary complexes, although the 1:2:1 and 1:2:2 ternary complexes showed appreciable photocytotoxicity at a fluence higher than 2.7 J cm^{-2} (see Supplementary Information, Fig. S2A). Furthermore, when HeLa cells were incubated with the ternary complexes for a prolonged period (that is, 24 h) before photoirradiation, the results were similar to those in Fig. 3a (see Supplementary Information, Fig. S2B). The effect of PCI-mediated transfection was comparable to or more effective than that of hydroxychloroquine, a potent endosomotropic agent[21], depending on the cell lines (see Fig. 3a and Supplementary Information, Fig. S2A).

The effect of the ternary complex on the PCI-mediated transfection was further compared with that of $AlPcS_{2a}$ (aluminium phthalocyanine with two sulphonate groups on adjacent phthalate rings), which was demonstrated to be an effective photosensitizer in PCI[8–10]. Figure 3b shows the effect of $AlPcS_{2a}$ on the transfection efficiency of the pDNA/CP_4 polyplex (N/P ratio = 2) and cytotoxicity to HeLa cells with varying concentrations of $AlPcS_{2a}$ and fluence. In the system using $AlPcS_{2a}$, the photochemical enhancement of the transfection was accompanied by a significant increase in the photocytotoxicity, regardless of the concentrations

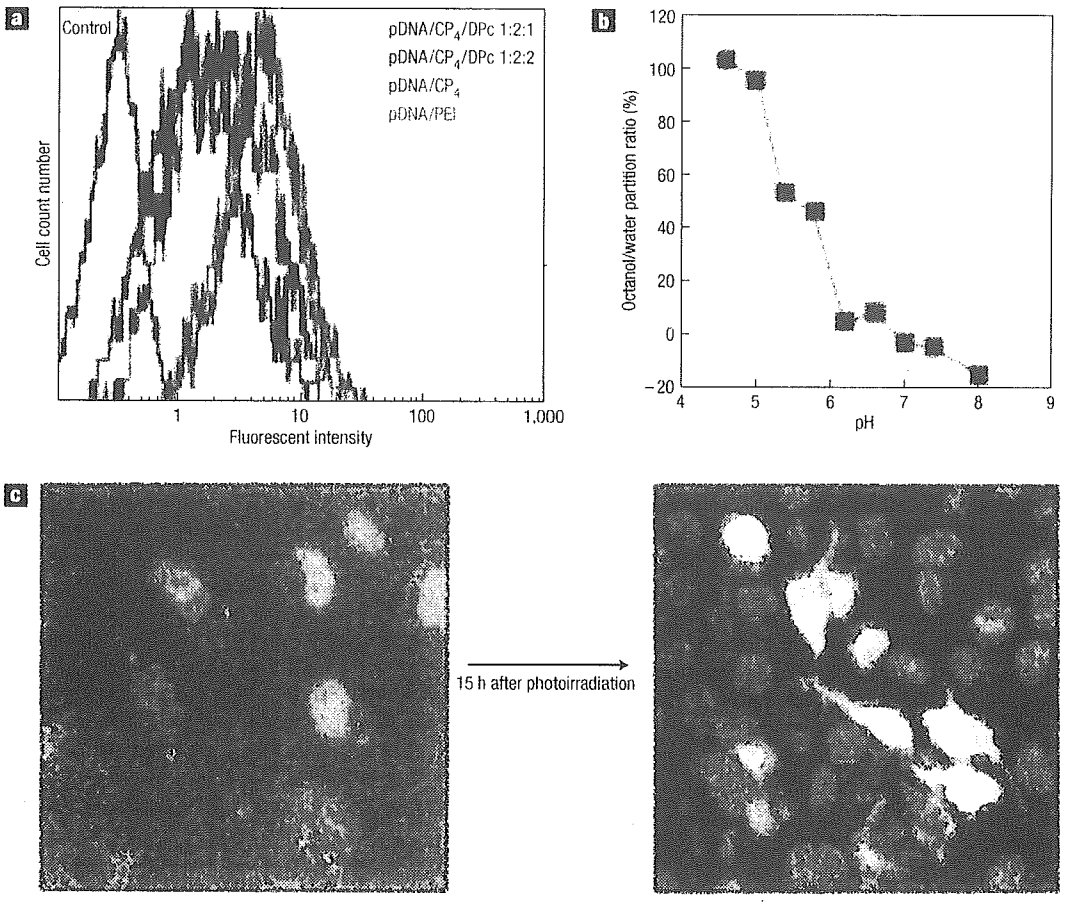

Figure 2 Properties of DPc and the pDNA/CP_4/DPc ternary complexes. a, Cellular uptake of the electrostatic complexes incorporating fluorescein-labelled pDNA. HeLa cells were incubated with each complex for 6 h, followed by flow cytometric analysis. The pDNA/PEI polyplex was prepared at an N/P ratio of 10. **b**, The pH-dependent partitioning (%) of DPc from the aqueous phase to the octanol phase. **c**, The intracellular distribution of FITC-dextran (green) co-incubated with the pDNA/CP_4/DPc complex with a charge ratio of 1:2:1 before and after photoirradiation. HeLa cells were incubated with the ternary complex for 6 h, followed by photoirradiation. The cell nuclei were stained with Hoechst 33258 (blue).

of $AlPcS_{2a}$. Comparison between Fig. 3a and b reveals that the ternary complex achieved an expanded range of safe light doses, in which remarkable photochemical enhancement of the transgene expression was accomplished without compromising cell viability, ensuring the safety and effectiveness of the PCI-mediated *in vivo* gene delivery.

The reduced cytotoxicity after prolonged incubation with synthetic vectors might be one of the main criteria for successful *in vivo* transfection. In this study, the cells were photoirradiated after 6 h incubation with each complex, followed by 48-h post-incubation without medium replacement. Figure 3c shows the transfection efficiency and cytotoxicity of each complex after prolonged incubation. The 1:2:0.5, 1:2:1 and 1:2:2 ternary complexes showed 158-, 117- and 23-fold photochemical enhancement of the transfection, respectively, with approximately 20% decreases in the cell viability. In contrast, the efficient transfection by the PEI polyplex was accompanied by a remarkable decrease (~85%) in the cell viability. Thus, the PCI-mediated gene delivery can avoid long-term toxicity, which is often induced by the polyplexes based on buffering polycations, because the process toxic to the cell is controlled in a light-responsive manner. Also, the ternary complex with a negative ζ-potential value might hardly interact with the negatively charged cell membranes, leading to reduced cytotoxicity in long-term incubation.

The potential of the ternary complex for *in vivo* PCI-mediated gene delivery was studied by the transfection of a reporter gene (a variant of yellow fluorescent proteins, Venus) to the conjunctival tissue in rat eyes on laser irradiation. In this study, the rat eyes received a subconjunctival injection of the ternary complex (360° circumferential to the cornea), and part of the conjunctiva was then irradiated with a semiconductor laser (689 nm) at 2 h post-injection (Fig. 4a). The pDNA/CP_4/DPc ternary complex with a charge ratio of 1:2:1 achieved significant gene expression only at the laser-irradiated site in the conjunctiva in 8 out of 12 eyes (2 days after irradiation) (Fig. 4b,c). Neither the ternary complexes with different compositions (that is, the 1:2:0.5 and 1:2:2 ternary complexes) nor ExGen500, which is one of the most efficient synthetic vectors, showed visible transgene expression. With the passage of time, the number of transfected eyes as well as the fluorescent intensity significantly decreased (Fig. 4c). Fluorescent microscopic observation of a frozen section of the conjunctival tissue revealed that the conjunctival epithelial cells were clearly transfected (Fig. 4d,e). Thus, the transfection only at the laser-irradiated site in the conjunctival tissue was achieved by the PCI-mediated gene delivery using the ternary complex. To our knowledge, this is the first success in PCI-mediated gene delivery *in vivo*.